Dual-Phase Steels Modeling – A Strain Gradient Approach

E. A. Bonifaz, PhD
Departamento de Ingeniería Mecánica de la Universidad San Francisco de Quito, Casilla Postal: 17-12-841 Círculo de Cumbayá, Quito, Ecuador, edisonb@usfq.edu.ec

J. Gil Sevillano, PhD
CEIT, Paseo de Manuel Lardizábal, 15, 20018 San Sebastián y Escuela Superior de Ingenieros, Universidad de Navarra, Aptdo. 1674, 20080 San Sebastián – Spain, jgil@ceit.es

Abstract
To obtain the behaviour of dual-phase microstructures, a three-dimensional (3D) strain gradient finite element model has been developed. The effect of grain size on flow stress has been investigated in polycristalline dual-phase steels. A strong size-dependence of plastic deformation in the micron range is observed. To describe the work hardening process in polycrystalline materials, two models, a gradient-one-internal-variable model and a gradient-total dislocation density evolution model, constructed in the basis of the Kocks-Mecking model are proposed. Results demonstrate that more dislocations are stored in specimens with finer grains and that the total dislocation density is not a single function of strain. Ferrite and martensite individual mechanical behaviour calculated into the dual-phase composite structure are presented. The effect of plastic deformation gradients imposed by the microstructure is clearly observed. An attempt is made to determine the mathematical expressions which best describe the strain hardening behaviour of crystalline materials in uniaxial deformation.

Keywords
Strain gradient plasticity, size effect

1. Introduction

As a point of departure, we will discuss the specific relation between flow stress and dislocation density that is in common usage. According to the experimental observations carried out by Narutani and Takamura [1] and other investigators [2-4], the flow stress is proportional to the square root of dislocation density ρ irrespective of the grain size, amount of strain and test temperature. For a coarse-grained single-phase material, which can be regarded as "structureless", the flow stress at zero temperature is set equal to

$$\sigma = M\alpha Gb\sqrt{\rho} \qquad \sigma = \hat{\alpha} Gb\sqrt{\rho} \tag{1}$$

Here M is the average Taylor factor, which evolves in the process of straining (in what follows, M will be considered constant for simplicity), b is the magnitude of the Burgers vector, G an appropriate shear modulus and $\hat{\alpha}$ a constant of order unity which depends, in part, on the strength of the dislocation/dislocation interaction [5]. Thermal activation may lower this effective obstacle strength so that the flow stress at a finite temperature and strain rate becomes

$$\sigma = s(\dot{\varepsilon}, T)\,\hat{\alpha} Gb\sqrt{\rho} \tag{2}$$

Where $s(\dot{\varepsilon},T)$ is a function that goes to 1 as T$\rightarrow$ 0. From eq (2) it is apparent that the flow stress is a product of a rate sensitivity term and a structure sensitive term. The flow stress as given by eq. (1) and (2) relates only to the impediment to dislocation motion that is provided by other dislocations. In most materials, there are other contributions to the plastic resistance. In some cases (e.g., lattice resistance, solution hardening, some grain size effects), these are additive to the contributions discussed above [5]

$$\sigma = \sigma_0(\dot{\varepsilon},T) + \hat{\alpha}(\dot{\varepsilon},T)Gb\sqrt{\rho^T} \tag{3}$$

Here, the rate dependence of σ_o may be more important than that of $\hat{\alpha}$ (or s), or it may be negligible; the less rate sensitive term (contained into the σ_o term) is often called an "internal stress" (Pierls or friction stress). The total dislocation density ρ^T is defined by Ashby [4] as the sum of geometrically necessary dislocations ρ^G and statistically stored dislocations ρ^S. The statistically stored dislocations are accumulated in pure crystals during straining and are responsible for the normal 3-stage [4]. On the other hand, the difference in crystallographic orientation between neighbouring grains can be corrected by introducing geometrically necessary dislocations, which are introduced to accommodate the incompatibility of deformation between grains.

To illustrate the above definition, consider the tensile deformation of a polycristal or of a two-phase alloy in which both phases are able to deform. If each grain deforms in a uniform manner, overlap and voids appear, because the two phases (or neighbouring grains) are not equally easy to deform. One component deforms less than the other, or not at all, so that gradients of deformation form with a wavelength equal to the spacing between the phases or particles [4]. Such alloys are plastically non-homogeneous, because gradients of plastic deformation are imposed by the microstructure. The geometrically necessary dislocations are stored in them to accommodate the deformation gradients, and so allow compatible deformation of the two phases. Note that, since each grain was deformed uniformly, the statistically dislocation density ρ^S and the state of work hardening within it must be the same as that of an "equivalent single crystal", i.e. a single crystal so oriented that it deforms on the same slip system or systems as the grain under consideration [4]. Ashby`s total dislocation density ρ^T definition assume that the geometrically necessary dislocations, ρ^G, have no direct influence on the accumulation of the statistically stored dislocations ρ^S.

1.1 Nature of statistically stored dislocations

As mentioned above, the statistically stored dislocations are related with strain hardening process. Strain hardening (or work hardening) is caused by dislocation interacting with each other and with barriers that impede their motion through the crystal lattice (mutual trapping during the deformation of the matrix). It is believed to occur when dislocations moving in the slip plane cut through other dislocations intersecting the active slip plane. The dislocations threading through the active slip plane are often called a dislocation forest. It is known that the number of dislocations in a crystal increases with strain over the number present in the annealed crystal [6]. Dislocation multiplication can arise from condensation of vacancies, by regeneration under applied stress from existing dislocations by either the Frank-Read mechanism or a multiple cross-slip mechanism or by emission of dislocations from a high-angle grain boundary [6].

2. Dislocation density-related constitutive modeling

The step of translating from the simple dislocation equations to a continuum formulation is not obvious. The statistically stored dislocations ρ^S are assumed to be dependent on the plastic strain ε^p, while the geometrically necessary dislocations ρ^G are assumed to be dependent on strain gradient $\partial\varepsilon^p / \partial x$ [7] or in a linear manner with the reciprocal of the grain size [1, 4]. The effect of grain size on flow stress has been investigated by Narutani and Takamura [1]. In their nickel dislocation density measured by resistivity studies, it was found that the dislocation density ρ^G for a given strain in

specimens deformed in tension at 77 and 295 K increases in a linear manner with the reciprocal of grain size, and that the statistically stored dislocations ρ^S are function of the equivalent strain ε_{eq}.

In its present state, dislocation density-related constitutive modeling it is considered mature enough to be broadly used in finite element codes including viscoplasticity [8]. In order to formulate the grain-size dependence of the total dislocation density, it is necessary to derive an equation to describe the accumulation of dislocations during deformation, but the constitutive equation to describe the work hardening process in polycrystalline materials has not been well established. The flow stress dependence on a rate sensitivity term and on a structure sensitive term (include lattice resistance and solution hardening) is accounted in equation (3). For the purpose of this paper, we assume that σ identifies only the dislocation/dislocation interaction component of the flow stress through the evolution of the ρ term. Lattice resistance and solution hardening are accounted in the σ_0 term.

$$\sigma = \sigma_0 + M\alpha Gb\sqrt{\rho^T} \tag{4}$$

To describe the work-hardening process in polycristalline materials, two models constructed in the basis of Kocks-Mecking model are presented. Here, we only examine the results obtained using the gradient total dislocation density evolution model (GM2) explained in section 2.2.

2.1 The gradient-one-internal-variable model (GM1)

This model is constructed on the basis of the following equations:

$$\sigma = \sigma_0 + M\alpha Gb\sqrt{\rho^S + \rho^G} \tag{5}$$

$$\rho^S = \left[\frac{K_1}{K_2}\left(1 - e^{\frac{-MK_2\varepsilon}{2}}\right) + \sqrt{\rho_0}\, e^{\frac{-MK_2\varepsilon}{2}}\right]^2 \tag{6}$$

$$\rho^G = C\frac{\chi_{eq}}{b} \tag{7}$$

Here, M , ρ^G , ρ^S , and others were defined in the preceding, C is a constant ranging from 1 to 2, χ_{eq} represents the magnitude of the curvature tensor $\boldsymbol{\chi}$ used as the scalar measure of the density of geometrically necessary dislocations ρ^G [9]

$$\chi_{eq} = \sqrt{\frac{2}{3}\chi_{ij}\chi_{ij}}$$

$\chi_{ni} = e_{nkj}\varepsilon_{ij,k}$

e_{nkj} = the alternating tensor

$\varepsilon_{ij,k}$ = the strain gradient tensor

ρ_o = the initial dislocation density[1] (the number present in the undeformed crystal).

K_1 and K_2 characterise the processes of dislocation storage and concurrent dislocation annihilation by dynamic recovery, respectively [10]. The process of dislocation storage is athermal, so that K_1 is a constant. By contrast, the coefficient K_2 represents a thermally activated process of dynamic recovery

[1] At the last stage of processing dual phase material is intercritically annealed and afterwards cooled down very rapidly. During cooling the austenite transforms into martensite. The volume of the phase increase causing residual stress around the martensitic phase. As a consequence of this, distortion of the crystal is produced (in this work, distortion does not refer to the deformed crystal condition). In dual phase steels modeling, the ρ_o term can be used to represent the initial dislocation density that is present in each phase before straining.

by dislocation cross-slip (low temperature case) or dislocation climb (high temperature case). The boundary between the two temperature regimes lies at approximately two thirds of the melting temperature. In both cases, the strain rate and temperature dependence of K_2 can be expressed as follows [10]:

$$K_2 = K_{20}\left(\frac{\dot{\varepsilon}^p}{\dot{\varepsilon}_0^*}\right)^{-1/n} \tag{8}$$

where K_{20} is a constant. The temperature dependence is contained either in n (in the low-temperature case when n is inversely proportional to temperature T, while $\dot{\varepsilon}_0^*$ can be considered constant) or in $\dot{\varepsilon}_0^*$ (in the high-temperature case when it is given by an Arrhenius-type equations, n being a constant ranging from 3 to 5).

In the present work we do not consider the temperature and strain rate dependence in K_2, so, the term associated with the dynamic recovery is assumed to be a constant. The identification of constants K_1 and K_2 are explained in section 3.

2.2 The gradient total dislocation density evolution model (GM2)

The variation of ρ^T in the process of plastic deformation can be described by an evolution total dislocation density model, and its respective constitutive equation:

$$\frac{d\rho_i^T}{d\varepsilon} = \frac{d\rho_i^G}{d\varepsilon} + \frac{d\rho_i^S}{d\varepsilon} \tag{9}$$

$$\left(\sigma_i - \sigma_0.\frac{M_i}{M}\right).\frac{d\sigma}{d\varepsilon} = \frac{1}{2}\left(M_i.\alpha.G.b\right)^2.\frac{d\rho_i^T}{d\varepsilon} \tag{10}$$

where,

$$\frac{d\rho_i^S}{d\varepsilon} = M_i.\left(K_1.\sqrt{\rho_i^T} - K_2.\rho_i^S\right)$$

$$\frac{d\rho_i^G}{d\varepsilon} \Leftrightarrow \textit{extrapolated from the previous increment}$$

For a polycristal the orientation factor M_i varies from grain to grain and it is also necessary to determine some average orientation factor M. Here, the subscript i refers to some specific grain. Details about the M_i term can be found in reference [11].

3. Parameter Identification

For a coarse-grained (or monocrystalline) single-phase material which can be regarded as "structureless", the evolution equation in the form of Eq. (11) describes materials where dislocation storage is controlled by the total dislocation density.

$$\frac{d\rho}{d\varepsilon} = M(K_1\sqrt{\rho} - K_2\rho) \tag{11}$$

Differentiation of Eq. (1) gives

$$\frac{d\sigma}{d\varepsilon} = \frac{1}{2} M\alpha Gb \frac{1}{\sqrt{\rho}} \frac{d\rho}{d\varepsilon} \tag{12}$$

Combining Eqs. (1), (11) and (12), the following equation can be derived.

$$\sigma \frac{d\sigma}{d\varepsilon} = \frac{1}{2} M^2 \alpha G b K_1 \sigma - \frac{1}{2} M K_2 \sigma^2 \tag{13}$$

$$\text{or} \qquad \sigma \frac{d\sigma}{d\varepsilon} = \theta_{II} \sigma - \frac{1}{2} M K_2 \sigma^2 \tag{14}$$

where,

$\theta_{II} = \frac{1}{2} M^2 \alpha G b K_1$ is the stage II hardening rate = the slope of the stress-strain curve in stage II.

It is recognized that θ_{II} is the limit value of the strain-hardening rate for $\sigma \to 0$. On the other hand, when σ approaches its saturation value σ_s, the strain hardening coefficient $\theta = (d\sigma / d\varepsilon)_{\dot{\varepsilon}} \to 0$. So, from Eq. (13)

$$\sigma_S = \alpha G b M \frac{K_1}{K_2} \tag{15}$$

and Eq. (14) can also be expresed in the form

$$\theta = \theta_{II} \left(1 - \frac{\sigma}{\sigma_S} \right) \tag{16}$$

The constants K_1 and K_2 for a polycristalline material can be calculated if the value of the stage II hardening rate θ_{II} and the value of the saturation stress σ_s are estimated. In references [12,13] it is established that σ_s is independent of strain rate and varies from 0.6 to 3 x 10^{-2} G for different materials, the higher values being those for materials with a lower Stacking Fault Energy (SFE). According to Refs. [8,12], the work hardening rate θ_{II} which is almost independent of temperature or strain rate, ranges from 1/15 to 1/30 of the shear modulus G. In a recent work [11], the following expressions are documented:

$$\theta_{II} = \left(\frac{d\sigma}{d\varepsilon} \right)_{\sigma = \sigma_0 . \frac{M_i}{M}} = 4.5 \, M_i^{\,2} \frac{G}{1000} \tag{17}$$

$$\sigma_s = \sigma_0 \frac{M_i}{M} + 213 . M_i = \sigma_y + 213 . M_i \tag{18}$$

In absence of other expressions, the constants K_1 and K_2 calculated from a coarse-grained single-phase material basis, can be used in polycristalline materials.

$$K_1 = \frac{2.\theta_{II}}{M_i^{\,2} . \alpha . G . b} = \frac{0.009}{\alpha \, b} \tag{19}$$

$$K_2 = \frac{2.\theta_{II}}{\sigma_S . M_i} = \frac{0.009 G M}{\sigma_0 + 213 M} \tag{20}$$

Finally, by combining Eqs. (6), (11) and (12) we obtain the following strain dependent hardening rate equation:

$$\frac{d\sigma}{d\varepsilon} = \frac{1}{2} M^2 \alpha G b \left\{ K_1 - K_2 \left[\frac{K_1}{K_2} \left(1 - e^{-0.5 M K_2 \varepsilon} \right) + \rho_0^{1/2} e^{-0.5 K_2 M \varepsilon} \right] \right\} \tag{21}$$

Equation (21) will be used to compare the effect of geometric obstacles that are present in non-homogeneous alloys. In other words, it will be used to observe the effect of plastic deformation gradients imposed by the microstructure.

4. Finite Element Modelling

To represent a real dual-phase microestructure, the virtual microestructure generator RANVORJM [14] has been used. The principle of the microstructure generator can be explained in short: In a cubic volume, a given number of nuclei is generated with random positions inside the cube. The formation of grains is simulated through the simultaneos "growth" of the nuclei. The growth is stopped-locally when a grain encounters another one. Finally, the grains are randomly distributed into the two (or several) phases, with prescribed proportions. In the present study, the martensite/ferrite grain size ratio ($R = D_{martens}/D_{ferrite}$) is conveniently generated to reproduce real dual-phase microestructures. The calculations are performed with the ABAQUS [15] FEM code. The finite element mesh is representative of the considered volume. The two-phases were uniformly meshed with cubic 8 node (C3D8) elements. The mechanical behaviour of each phase is assumed be represented by the above constitutive equations with appropriate values.

The macroscopic stress σ and strain ε in the traction direction are deduced from the resulting force on the face where the displacement is applied (for the stress) $\sigma = \frac{1}{A}\int_A \sigma_{22} dA$ and from the displacement itself (for the strain) $\varepsilon = \ln\left(1 + \frac{u_2}{l_0}\right)$.

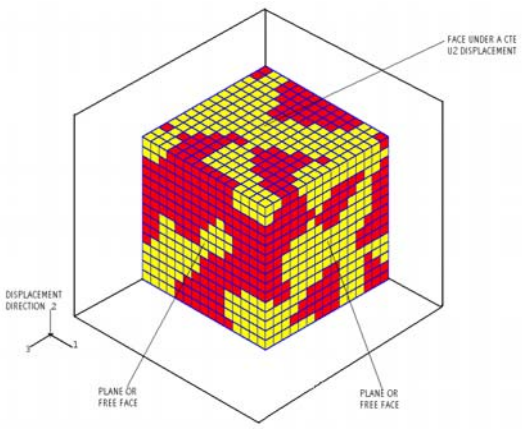

Figure 1: Element mesh and boundary conditions for FEM model.

To model a gradient plasticity theory using ABAQUS, we use the URDFIL subroutine to read the quantities that output in the results file. In particular, we read the strains at each Gauss integration point at the end of an increment, and calculate the strain gradient function from the previous increment (not current strain gradients). For further calculations, the strain gradients are passed into UMAT routine through a common block.

5. Results and Discussions

A Finite Element (FE) calculation was carried out for a 24 % martensite dual-phase steel using the ABAQUS implementation of the model, with parameters documented in Part I and section 3 of the present study. The results of this simulated test were then compared with actual experimental data. This comparision, shown in Figure 2 demonstrates good agreement between experiment and model prediction (which, however, became less satisfactory at large elongations). The reason could be attributed to the number of other effects not included in the simulation, e.g , strain rate or temperature)

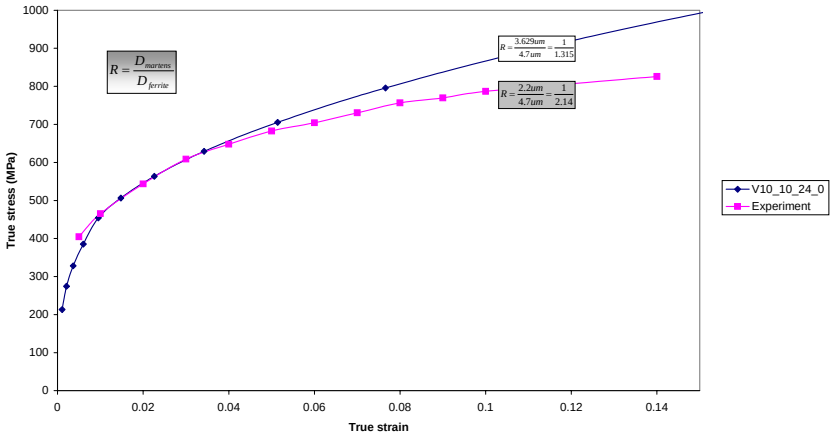

Figure 2: Uniaxial stress vs strain for a 24% martensite dual-phase steel. Simulation parameters: σ_o^f =248 Mpa, σ_o^m = 1342 Mpa, %CT = 0.08, %CF = 0., %CM = 0.3416, G = 83.077 Gpa, ν = 0.3, b = 0.25E-3 *um*, α = 0.2, M = 2.83, M_i (according to a square distribution), ρ_o= 1 cm^{-2}, 12 grains (1000 elements C3D8), plane faces.

A hardening rate- stress diagram (Figure 3) for ferrite and martensite phases are clearly reproduced by the total dislocation evolution model. It is observed the strong grain size dependence calculated by introducing the strain gradient contribution into the mechanical behaviour ferrite and martensite constitutive equations. It is important to note that these curves represent the θ-σ individual behaviour of single phases into the dual-phase composite structure. The results are obtained in element number 4 of grain FERRI03 (the name of one of the 12 grains used in the model) for the ferrite and in element 3 of grain MARTE01 for the martensite.

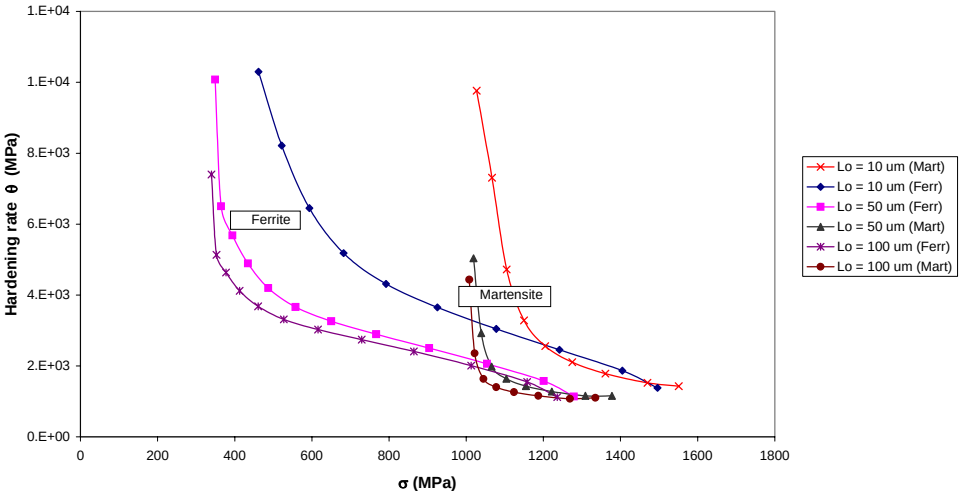

Figure 3: The ferrite and martensite θ-σ diagram. Values calculated in element 3 of grain MARTE01 for the martensite, and element 4 of grain FERRI03 for the ferrite. The effect of grain size on the strain hardening rate θ calculated at a maximum true strain of 0.3.

To quantify the size effect which cannot be predicted with conventional plasticity theories, Figure 4 shows a set of experiments displaying strong size dependence of plastic deformation in the micron range. The plot brings out the increased effective strength of the smaller 10 *um* specimen initial length.

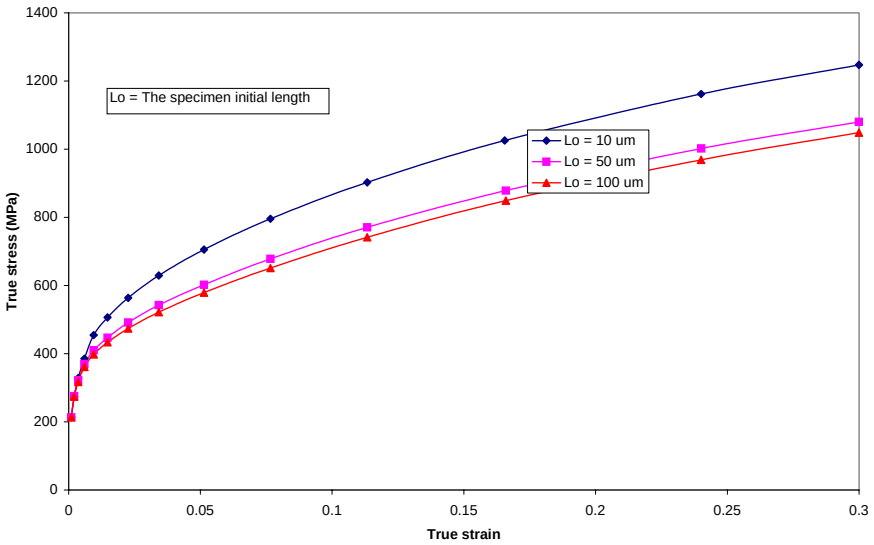

Figure 4: The flow stress-grain size dependence in a 24% martensite dual phase steel. Simulation parameters documented in Figure 1.

The results plotted in Figure 5 suggest that more dislocations are stored in specimens with finer grains and that the total dislocation ρ^T is not a simple function of strain. The difference between ferrite and martensite total dislocation behaviour can be atributted to differences in yield stress and Taylor orientation factor which varies from grain to grain. It is important to note that either the ferrite or martensite initial dislocation density ρ_o are not included in the simulations, however, that contribution can easily be implemented.

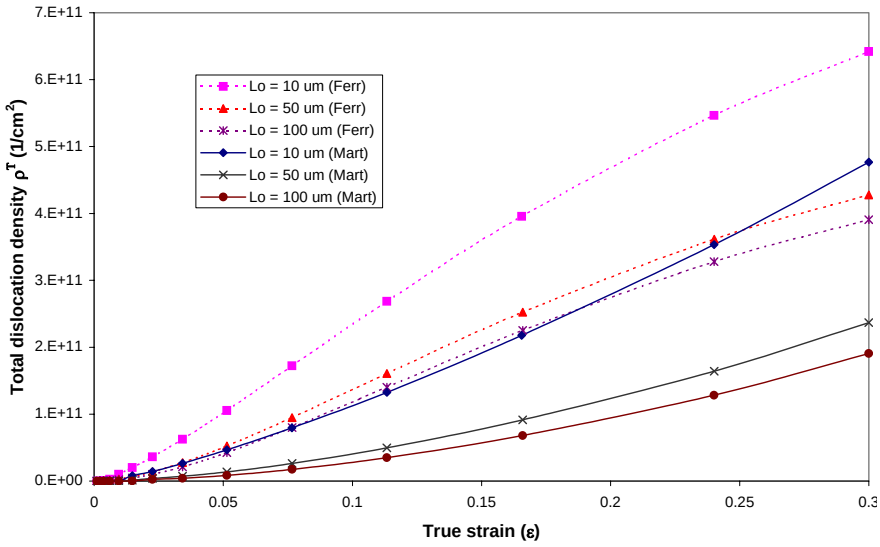

Figure 5: Ferrite and martensite total dislocation density as a function of true strain.

Figures 6 and 7 show the effect of geometric obstacles that are present in polycristalline materials (non-homogeneous alloys). The effect of plastic deformation gradients imposed by the microstructure is clearly observed. It is interesting to note that at large elongations, the curves tend to fall on top of one another.

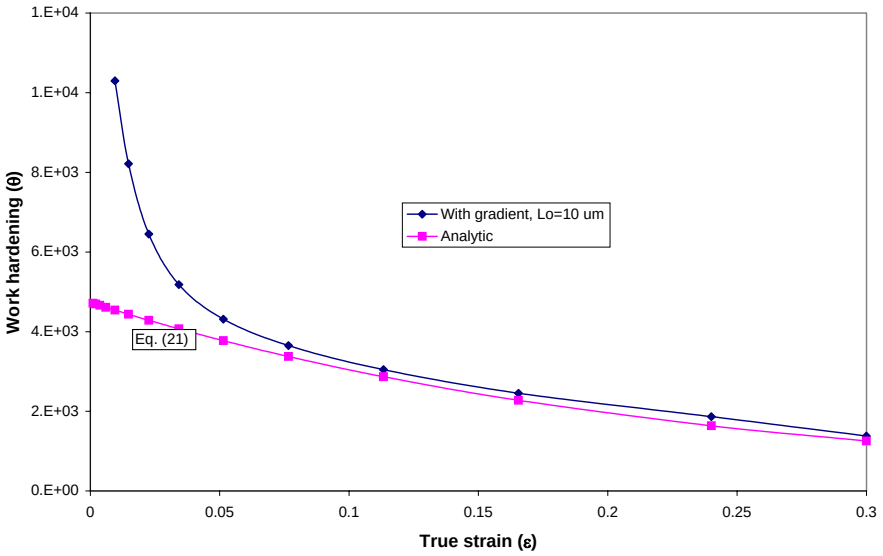

Figure 6: The effect of strain gradient on the θ-ε curve. Values calculated for the ferrite single phase in element 4 of grain FERRI03.

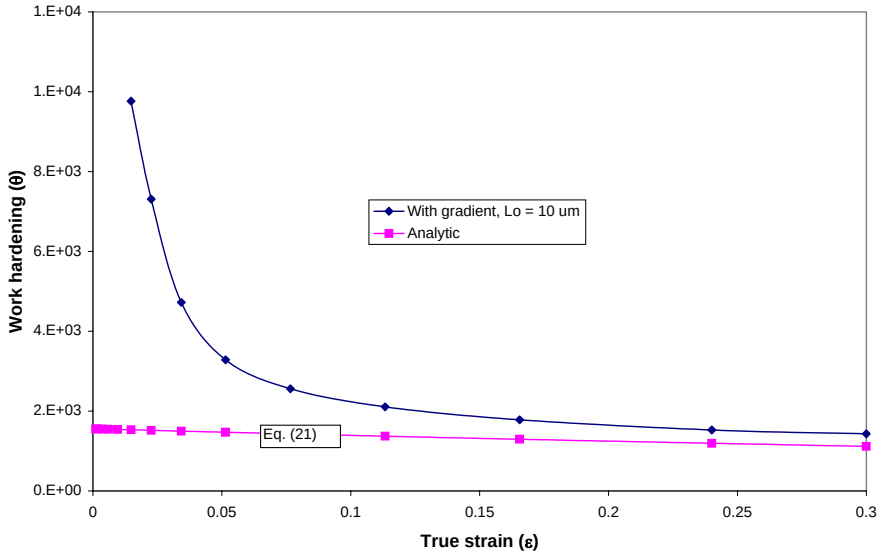

Figure 7: The effect of strain gradient on the θ-ε curve. Values calculated for the martensite single phase in element 3 of grain MARTE01.

Knowing the mechanical response of the coarse-grained material through equation (14), one can estimate the behavior of a grain-refined one. This becomes clearer if the stress dependence of the strain hardening is plotted in a particular type of $\theta\sigma$-σ diagram [8]. Figures 8 and 9 show the grain size effect on strain hardening as seen in the $\theta\sigma$-σ diagram for polycrystalline martensite and ferrite respectively. The coarse grained (matrix) is represented by an inverted parabola intersecting the abscissa at $\sigma = 0$ and $\sigma = \sigma_s$. A parallel shift of the parabola along the ordinate axis by an amount inversely proportional to grain size is observed. The inverted parabola behavior deviation observed in

the martensite case (fig. 8), it is atributted not only to the non-homogeneous plastic deformation imposed by the microstructure (volume fraction morphology) but also to the ferrite/martensite interaction (different Taylor orientation factor) and boundary conditions constrains (position of elements 3 and 4 into the FEM grid). One component deforms less than the other, or not at all, so that gradients of deformation form with a wavelength equal to the spacing between the phases or grains.

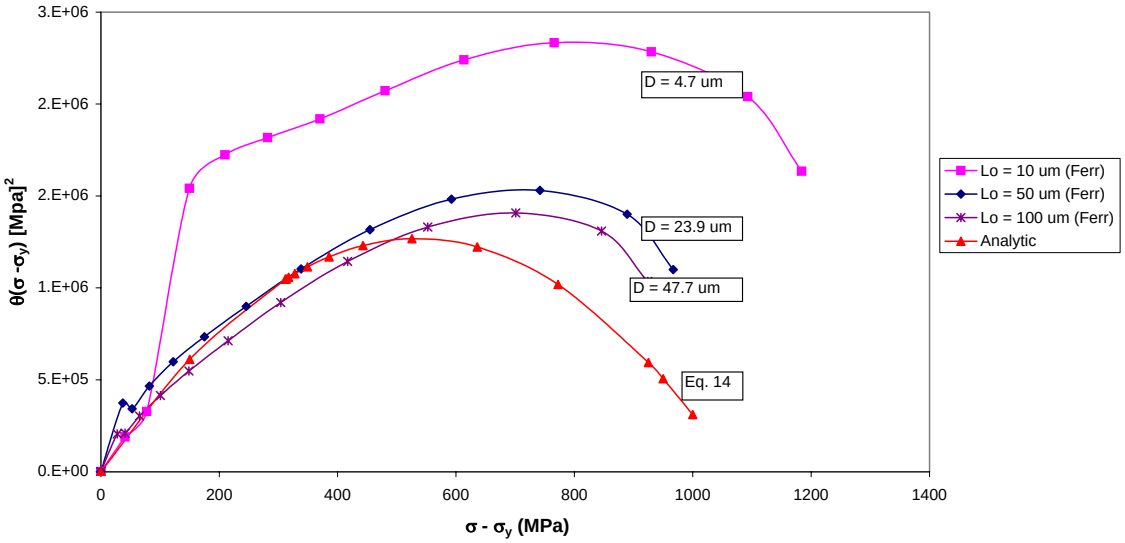

Figure 8: The martensite $\theta\sigma$-σ diagram in a 24 % martensite dual phase steel.

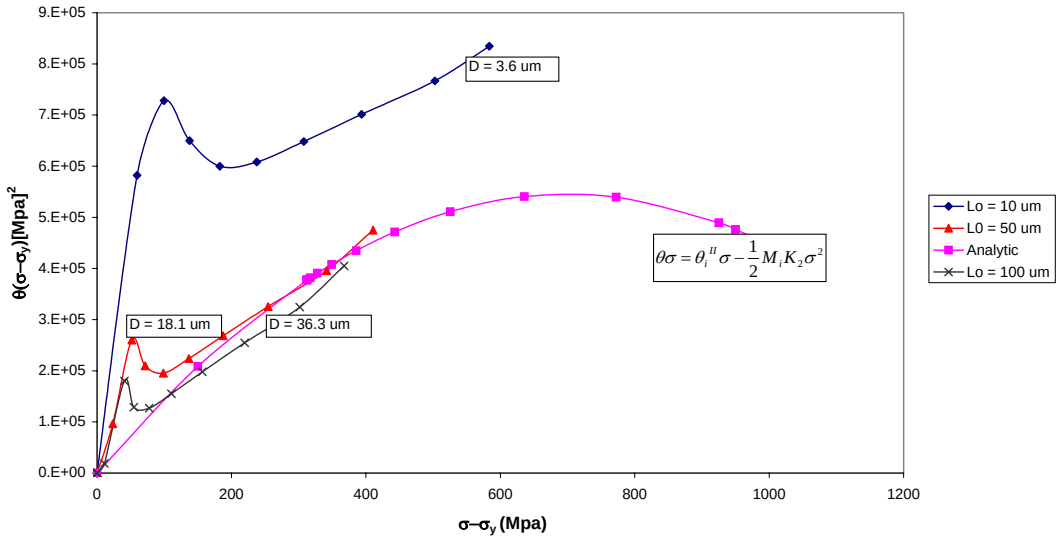

Figure 9: The ferrite $\theta\sigma$-σ diagram in a 24 % martensite dual phase steel.

Figure 10 shows the effects of work hardening rate on the maximum uniform elongation during tensile straining. Differences in ferrite and martensite work hardening behaviour are clearly observed.

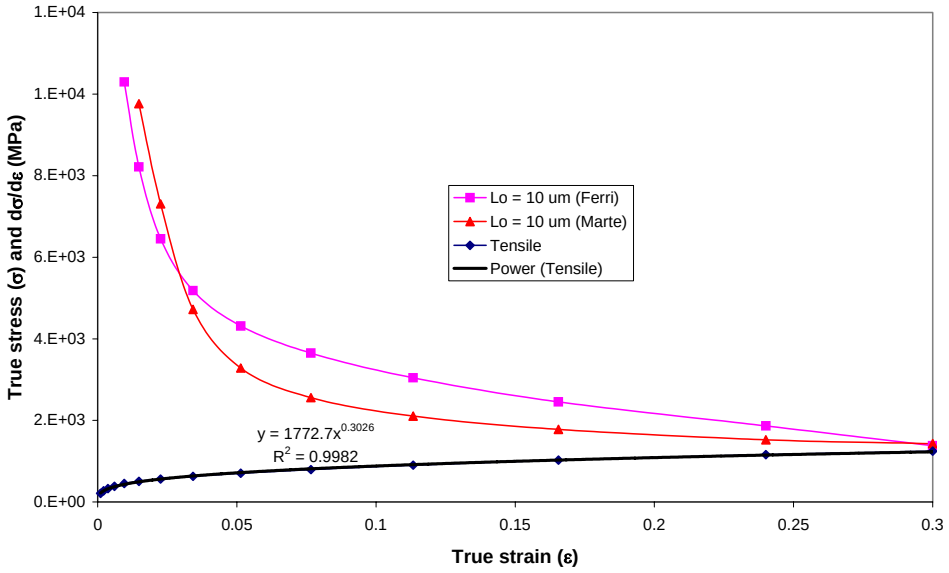

Figure 10: True stress σ and work hardening rate θ - true strain (ε) diagram. Values calculated in element 3 of grain MARTE01 for the martensite, and element 4 of grain FERRI03 for the ferrite.

6. Conclusions

The effect of grain size on flow stress was investigated for polycristalline dual phase using the gradient- total dislocation density evolution model.

Mechanical behaviour of ferrite and martensite single phases calculated into the dual-phase composite structure is presented.

The increase in effective strength of the smaller specimens in tension is due to strain gradients deformation. Components deform less than the other, or not at all, with a wavelength equal to the spacing between the phases or grains, as a matter of fact, an important number of geometrically necessary dislocations are produced.

It is shown that at large elongations, the individual polycrystalline single phase work hardening approximates the work hardening coarse grained (monocrystal) behaviour (eq. 21), i.e., the curves tend to fall on top of one another.

The effect of plastic deformation gradients imposed by the microstructure is clearly observed.

Results demonstrate that more dislocations are stored in specimens with finer grains and that the total dislocation density is not a single function of strain.

References

1. Narutani T., and Takamura. (1991). “Grain-size strengthening in terms of dislocation density measured by resistivity”. *Acta Metall. Mater.* Vol 39, Nº 8, pp. 2037-2049.

2. Meakin J. D. and Petch N. J. (1974). “Strain hardening of polycrystals: the α-brasses”. *Phil. Mag. 30*, 1149.

3. Dingley D. J. and McLean D. (1967). “Components of the flow stress of iron”. *Acta Metallurgica*, vol. 15.

4. Ashby M. F. (1970). “The Deformation of Plastically Non-homogeneous Materials”. *Phil. Mag*. 21, 399.

5. Mecking H. and Kocks U.F. (1981). “Kinetics of flow and strain-hardening”. *Acta Metallurgica* vol. 29, pp. 1865 to 1875.

6. Dieter G. E. (1986). *Mechanical Metallurgy*, McGraw-Hill International Book Company.

7. Hutchinson J. W. (2000). “Plasticity at the micron scale”. *International Journal of Solids and Structures* 37 225-238.

7. Estrin Y, in: A.S. Krausz, K. Krausz (Eds.). (1996). Unified Constitutive Laws of Plastic Deformation, Academic Press, N.Y., p 69.

9. Fleck N. A., Muller G. M., Ashby M. F. and Hutchinson J. W. Strain Gradient Plasticity: Theory and experiment. *Acta metall. Mater.* Vol 42, Nº 2, pp 475-487.

10. Estrin Y. (1994). “Dislocation theory based constitutive modelling: foundations and applications”. *Journal of Materials Processing Technology* 80-81 (1998) pp. 33-39.

11. Modelling of mechanical properties and local deformation of high strength multi-phase steels. *ECSC Steel RTD Annual Report*, March 2000.

12. Gil Sevillano J., Van Houtte, P. and Aernoudt E. (1980). *Prog. Mat. Sci*. 25, 69

13. Kocks, U.F. (1976). *J. Engng. Mater. Tech*. 98, 76.

14. Programa RANVORJM (1998), Centro de Estudios e Investigaciones Técnicas de Gipuzkoa (CEIT).

15. ABAQUS User´s Manual 5.8, Hibbit, Karlsson and Sorensen. (1998).

Biographic Information

Dr. Edison BONIFAZ CONTO. Dr. Bonifaz Conto is Professor of Materials Engineering, Physical Metallurgy of Welding and Numerical Analysis in the Mechanical Engineering Department at University San Francisco de Quito-Ecuador.

Dr. Javier GIL SEVILLANO. Dr. Gil Sevillano is Professor of Materials Science and Head in the Department of Materials Engineering (TECNUM, University of Navarra-Spain) and Department of Materials, CEIT (Centro de Estudios e Investigaciones Técnicas de Guipúzcoa).

Authorization and Disclaimer